Proceedings of the 17th World Congress
The International Federation of Automatic Control
Seoul, Korea, July 6-11, 2008

The Artificial Muscle as an Innovative Actuator in Rehabilitation Robotics

M. Knestel * **E.P. Hofer** * **S. Klee Barillas** * **R. Rupp** **

* *Institute of Measurement, Control, and Microtechnology, University of Ulm, 89081 Ulm, Germany,* {*markus.knestel, eberhard.hofer, sebastian.klee*}*@uni-ulm.de*
** *Orthopedic University Hospital II, 69118 Heidelberg, Germany, ruediger.rupp@ok.uni-heidelberg.de*

Abstract: This paper presents the application of artificial pneumatic muscle actuators in a novel motorized orthosis for an intensive home-based gait training in patients with neurological disorders. Owing to the inherent elasticity of these actuators, they are an ideal choice in realizing a soft and tractable assistance to aid the physiological movements of the lower extremities. Special focus is paid to the modeling of the dynamic nonlinear force characteristics of the muscles as a steerable mass-damper system, and to the approximation of the variation of muscle volume under different operating conditions. The model description uses polynomial functions for which coefficients are identified by minimizing a quadratic performance index. Based on the mechanical model of the knee joint of the apparatus, a nonlinear stability-oriented backstepping control supported by observer-based disturbance compensation is derived and applied to the prototype of the rehabilitation robot.

1. INTRODUCTION

The ability to walk is one of the most obvious attributes of human life. In patients with lesions of the central nervous system, particularly spinal cord injuries (SCI) or stroke, this ability is impaired to a more or less extent. In case of incomplete lesions with some preserved motor functions in the lower extremities several clinical trials have shown, that an intensive gait training leads to an essential improvement in gait capacity. This is mainly due to the enhancement of neural plasticity either in the spinal cord or the brain by the generation of physiologic afferent stimuli. Over the last decade, body weight supported treadmill training (BWSTT) has been established as a very effective tool to apply a sufficient training intensity in terms of step repetitions [Dietz et al. (1995), Hesse et al. (1995)]. During the BWSTT, the patients are put in a harness for body weight unloading and - in patients with weak muscles - their step movements are manually assisted by up to three therapists. In the last few years, first steps towards automation of BWSTT have been undertaken to free therapists from this considerably exhausting work [Colombo et al. (2001)]. Recent research work has investigated the influence and significance of afferent input from load receptors and joints in more detail [Dietz et al. (2002)]: comparable to some animal species, it has been found in spinal cord injured patients that the physiological movement of the hip joint and the appropriate gait-phase related loading and unloading of the foot soles are the key trigger sources of the spinal gait pattern generator. The aim of our present research is the development of an adjustable and modular motorized orthosis for gait training, which is operable in a sitting position and is capable of generating the key sensory stimuli mentioned above. Due to economical reasons, the primary rehabilitation period of patients in hospital is getting shorter and shorter. Since the therapeutically sufficient intensity of gait training cannot be maintained on an outpatient basis, the opportunity for operating the device at the patients' home has been explored as one of the most important design criteria. Therefore, artificial pneumatic muscles with their excellent weight-force ratio and price distributed by Festo AG, Germany, have been integrated as dynamic actuators to generate the movements of all the joints of the lower extremities. The artificial Fluidic Muscle is a vulcanised rubber hose strengthened by aramid fibers. Increasing the inner muscle pressure results in a longitudinal contraction combined with a concomitant expansion in the radial direction. The contraction causes a tensile force along the longitudinal direction. By antagonistic arrangement of the muscles, each movement can be realized. Two actuators of the type DMSP-20 are driving the knee joint via a cogwheel fixed to the knee axis. The ankle joint is driven by means of a rope-lever mechanism by muscles of the type

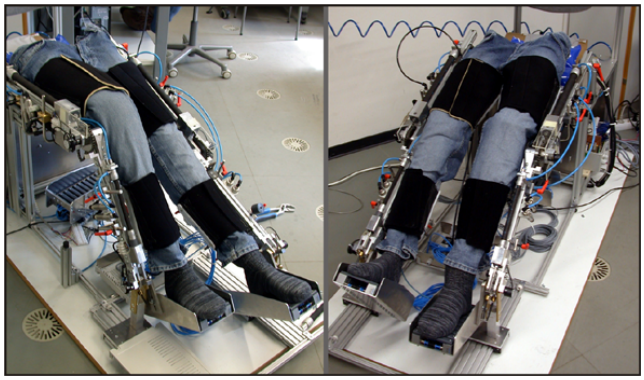

Fig. 1. Prototype of the rehabilitation robot for the lower limbs

978-1-1234-7890-2/08/$20.00 © 2008 IFAC

10.3182/20080706-5-KR-1001.3436

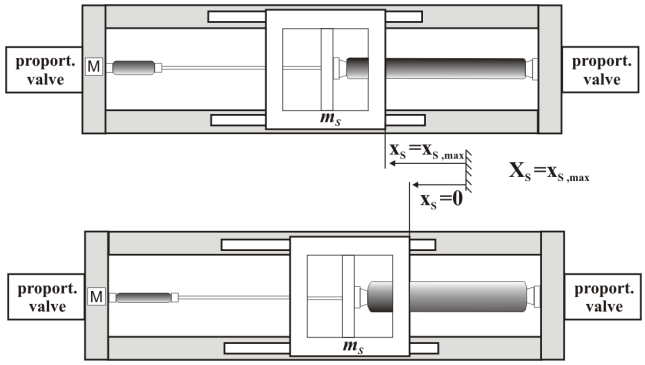

Fig. 2. Measurement setup for model identification

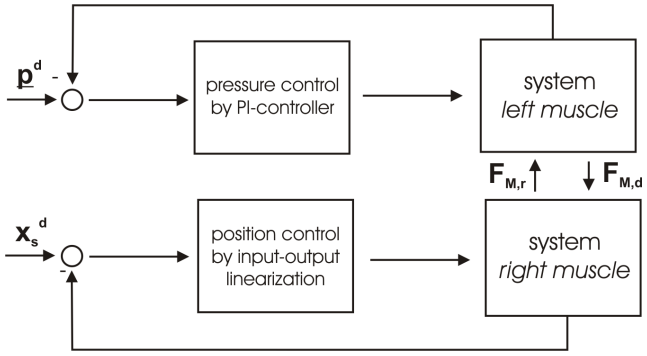

Fig. 3. Block diagram of the control configuration in the identification setup

MAS-10. While frequently used in industrial applications, only few rehabilitation applications using artificial muscles are known. Gordon et al. (2006) and Herr and Kornbluh (2004) have been utilized them in actuating an ankle-foot orthosis. In these studies, artificial muscles are used to provide single-joint support to the plantar flexion in different phases of gait, whereas here the antagonistic muscle actuation is supposed to track a physiological trajectory of the knee and ankle angle. To ensure stable tracking of the highly nonlinear system over a wide operating area at different velocities and conditions, nonlinear models of the muscles, pressure dynamics and mechanical dynamics are derived. The first functional prototype of the rehabilitation robot is depicted in fig. 1.

In this paper, the force and volume modeling of the pneumatic muscles is addressed first. Parts of the models are identified automatically by measurements in the test rig shown in fig. 2. Therefore, a nonlinear position control using exact input-output linearization is derived. In order to design a nonlinear position controller by backstepping for the knee joint, the mechanical model is computed by the use of Lagranges equations. A nonlinear observer with disturbance estimation ensures stable and accurate control.

2. MODELING OF THE FLUIDIC MUSCLE

2.1 Measurement Setup for Model Identification

The force and volume behavior in relation to the muscle contraction ΔL and the muscle pressure p_M, are identified with the measurement setup shown in fig. 2. On the right side, a forceful muscle of the type MAS-40 is responsible for the positioning of the carriage of mass m_S and causes the varying contraction of the left muscle. The muscle on the left is held on a constant pressure, while the position of the carriage is varied and the force at the position M is measured. The equation of motion for the carriage is given by

$$\ddot{x}_S = \frac{1}{m_S} \cdot [F_{M,d} - F_{M,r}(p_{M,r}, \Delta L_{M,r})] \ . \tag{1}$$

The force $F_{M,d}$ of the investigated muscle on the left is regarded as a disturbance. In contrast to $F_{M,d}$, the effects of friction and model uncertainties can be neglected. The contraction length $\Delta L_{M,r}$ is calculated according to fig. 2

$$\Delta L_{M,r} = X_S - x_S \ . \tag{2}$$

The pressure in the left muscle is adjusted by PI-control. The position controller is based on the theory of exact input-output linearization (fig. 3). The dynamics of the internal pressure in the muscle i can be obtained on the supposition of a polytropic, ideal process

$$p_{M,i} = p_0 \cdot \left(\frac{V_0}{V_{M,i}} \right)^n \ , \tag{3}$$

where p_0 is the barometric pressure, V_0 the volume of the environment and n the polytropic exponent for this process. The total derivation of (3) leads to

$$dp_{M,i} = \frac{\partial p_{M,i}}{\partial p_0} \cdot dp_0 + \frac{\partial p_{M,i}}{\partial V_0} \cdot dV_0 + \frac{\partial p_{M,i}}{\partial V_{M,i}} \cdot dV_{M,i} \ , \tag{4}$$

wherein the environmental pressure and volume have been regarded as constant. The ideal gas law is utilized to describe the thermodynamic behavior

$$p_{M,i} \cdot V_{M,i} = m \cdot R \cdot T_{M,i} \ . \tag{5}$$

The total derivation of (5) and the account of the muscle volume $V_{M,i}(\Delta L_{M,i}, p_{M,i})$ as a function of the contraction $\Delta L_{M,i}$ and the inner muscle pressure $p_{M,i}$ lead to

$$\begin{aligned} \dot{p}_{M,i} = & \frac{n}{V_{M,i} + n \cdot \frac{\partial V_{M,i}}{\partial p_{M,i}} \cdot p_{M,i}} [R \cdot T_{M,i} \cdot \dot{m}_{M,i} \\ & - \frac{\partial V_{M,i}}{\partial \Delta L_{M,i}} \cdot \frac{\partial \Delta L_{Mi}}{\partial x_S} \cdot p_{M,i} \cdot \dot{x}_S] \ . \end{aligned} \tag{6}$$

The system (1) can be transformed to state space with the states $x_1 = x_S$, $x_2 = \dot{x}_S$ and the output y

$$\begin{aligned} \dot{x}_1 &= x_2 \ , \\ \dot{x}_2 &= \frac{1}{m_S} \cdot [F_{M,d} - F_{M,r}(p_{M,r}, \Delta L_{M,r})] \ , \\ y &= x_1 \ . \end{aligned} \tag{7}$$

The force characteristics of the MAS-40 muscle as a polynomial fit of the measured force at variable pressure and constant contraction is borrowed from [Aschemann and Hofer (2004)]

$$F_{M,r} = F_{M,r}(\Delta L_{M,r}, p_{M,r}) \ . \tag{8}$$

The physical actuating variable u is the mass flow of air $\dot{m}_{M,r}$ into the muscle. In order to realize exact input-output linearization, the relative degree of the system δ has to be determined. The relative degree is equivalent to the number of differentiations of y required to obtain a dependency of the actuating variable u. With the time derivative of (8)

$$\dot{F}_{M,r} = \frac{\partial F_{M,r}}{\partial p_{M,r}} \cdot \dot{p}_{M,r} + \frac{\partial F_{M,r}}{\partial \Delta L_{M,r}} \cdot \Delta \dot{L}_{M,r} \ , \tag{9}$$

and the replacement of the derivative of the pressure $p_{M,r}$ by (6), the third derivative of the system output y is influenced by the actuating variable $u = \dot{m}_{M,r}$.

$$\begin{aligned} \dot{y} &= \dot{x}_1 = x_2 \ , \\ \ddot{y} &= \dot{x}_2 = \frac{1}{m_S} \cdot [F_{M,d} - F_{M,r}(p_{M,r}, \Delta L_{M,r})] \ , \\ \dddot{y} &= \frac{1}{m_S} \cdot \left[\underbrace{\dot{F}_{M,d}}_{\approx 0} - \dot{F}_{M,r}(u_{M,r}) \right] \ . \end{aligned} \tag{10}$$

Therefore, the relative degree of the system is $\delta = 3$. The derivative of the disturbance force generated by the left muscle is neglected. Alternatively, if better position tracking is desired, it could be estimated e.g. by a disturbance observer. Now, a control law that yields a linear differential equation relating a new input v and the output $y = x_1$ is of interest. Owing to a lack of space, the indices are neglected. With

$$\begin{aligned} u = & \frac{\left(-v \cdot m_S - \frac{\partial F}{\partial \Delta L} \cdot \Delta \dot{L}\right) \cdot \left(V + n \cdot p \cdot \frac{\partial V}{\partial p}\right)}{n \cdot R \cdot T \cdot \frac{\partial F}{\partial p}} \\ & + \frac{\left(n \cdot p \cdot \frac{\partial V}{\partial \Delta L} \cdot \frac{\partial \Delta L}{\partial x_S} \cdot \frac{\partial x_S}{\partial t}\right)}{n \cdot R \cdot T} \ , \end{aligned} \tag{11}$$

we obtain the linear input-output relationship. The error dynamics can be asymptotically stabilized by

$$\begin{aligned} v = & \dddot{x}_S^d + \alpha_3 \cdot (\ddot{x}_S^d - \ddot{x}_S) + \alpha_2 \cdot (\dot{x}_S^d - \dot{x}_S) \\ & + \alpha_1 \cdot (x_S^d - x_S) + \alpha_0 \cdot \int_0^t (x_S^d - x_S) d\tau \ . \end{aligned} \tag{12}$$

The coefficients $\alpha_k, k = \{0, ..., 3\}$, are determined by pole placement.

2.2 Force Behavior of the Fluidic Muscle

In order to describe the nonlinear force characteristics of the muscles in different operating states, a comprehensive model is needed. For this purpose, the muscle is considered as a controllable damped spring-mass oscillator, where the flexibility of the spring depends on the active contraction ΔL and the inner pressure p_M

$$F_M = \underbrace{c(\Delta L, p_M) \cdot \Delta L}_{F_{tow}} - \underbrace{D \cdot \frac{\partial}{\partial t} \Delta L}_{F_{damp}} \ . \tag{13}$$

The damping factor D is assumed to be constant, although in reality there exists an interdependency to ΔL and p_M. The reason for the omission is the use of a load cell in the measurement rig, which has a maximum preciseness of $50N$. The characterization of the tensile force F_{tow} leads to an approximately linear dependency of the muscle pressure p_M for both DMSP-10 and DMSP-20. The force dependency on the contraction ΔL is of a higher order. The towing force is partitioned into two terms

$$\begin{aligned} F_{tow} &= c(\Delta L, p_M) \cdot \Delta L = \overline{F}(\Delta L) \cdot p_M - f(\Delta L) \\ &= \sum_{j=0}^{3} (a_j \cdot \Delta L^j) \cdot p_M - \sum_{k=0}^{4} (b_k \cdot \Delta L^k) \ . \end{aligned} \tag{14}$$

The first term $\overline{F}(\Delta L)$ possesses a positive sign and represents an area function. The second term $f(\Delta L)$ with negative sign signifies a counterforce produced, in essence, by the fiber arrangement in the rubber hose.

2.3 Volume Behavior of the Fluidic Muscle

The muscles volume is approximated by a cylinder with two frustums at its ends. The total volume is obtained by adding the volumes of the partial bodies

$$V_M = V_{cyl} + 2 \cdot V_F \ . \tag{15}$$

On the assumption of a linear dependency between the frustums height h_F and the total length L, the volume can be calculated by only measuring the diameter D_{cyl} and the length L_{cyl} of the cylinder. The characterization measurements lead to two different assumptions for the DMSP-10 and the DMSP-20 muscle

$$V_{M10} = \sum_{i=0}^{1} (v_i^{M10} \cdot \Delta L^i) \cdot \sum_{j=0}^{2} (w_j^{M10} \cdot p_M^j) \ , \tag{16}$$

$$V_{M20} = \sum_{i=0}^{2} (v_i^{M20} \cdot \Delta L^i) \cdot \sum_{j=0}^{2} (w_j^{M20} \cdot p_M^j) \ . \tag{17}$$

2.4 Determination of the Damping Factor

As the muscle system represents a real vibratory system, the oscillation must be damped. In order to characterize the oscillatory behavior, the investigated muscle is held under constant pressure. The carriage is then pulled from its position of rest manually and released and this results in a near harmonic oscillation. The amplitude ratio of the two consecutive oscillations y_k and y_{k+1} is assumed to be constant

$$\frac{y_k}{y_{k+1}} = e^{\frac{D}{2 \cdot m} \cdot T_d} = constant \ . \tag{18}$$

The amplitudes y_k and y_{k+1} as well as the time T_d can be extracted out of the measured oscillation and the damping factor D can be computed. Indeed, the damping factor is also dependent on the muscle pressure and the contraction length. As the dynamic model error goes below the accuracy of the load cell, this interdependency has been neglected.

2.5 Model Identification

To determine the tensile force in relation to muscle pressure, contraction and contraction velocity, the test rig depicted in fig. 2 is used [Klee Barillas (2007)]. Generally, there are two different ways to vary the three interdependencies F_{tow}, ΔL and p_M. Either the contraction or the muscle pressure can be held constant, while the force is measured. Here, the alternative with constant pressure and variable contraction is employed, because it better emulates the application and shows lower hysteresis behavior. Thereby, the forces F_{tow} and F_{damp} will be determined separately. In order to vary the position of the carriage, a nonlinear position control using input-output linearization for the forceful MAS-40 muscle has been designed. The coefficients of the polynomial fitting (14), (16), and (17) are determined by minimization of a quadratic performance index (21). The identification procedure is as follows. A constant pressure between 2 bar and 7 bar is set by

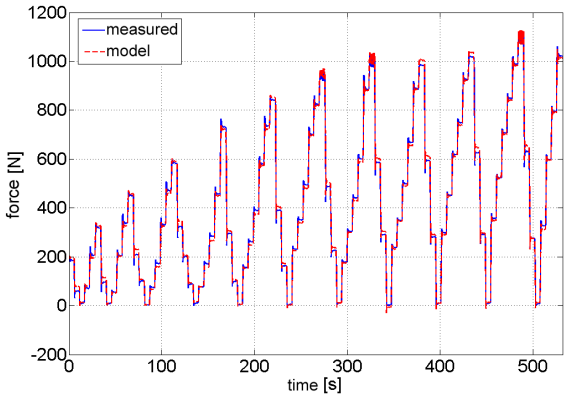

Fig. 4. Comparison of measured and calculated muscle force (DMSP-20)

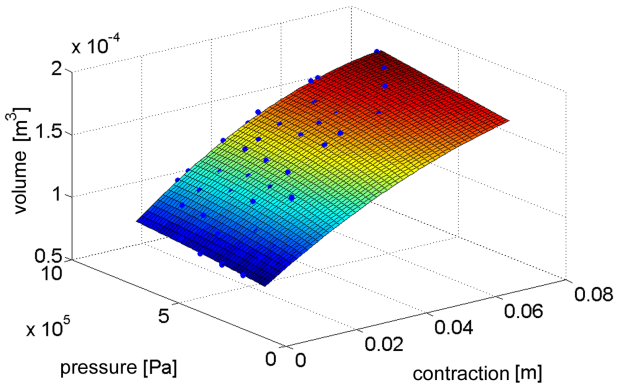

Fig. 5. Volume model (DMSP-20) with measuring points

the pressure control in the investigated muscle. Without any load, the elevated pressure effects a contraction. The position control on the right side stabilizes the position, where no force is measured. Next, the forceful muscle on the right tows the left muscle to zero contraction, while the pressure is held constant and the antagonized force is measured. The unknown coefficients a_j and b_k are wrapped up in the parameter column vector $\underline{\theta}$. In vector notation, the model force $\underline{F}_M$ can be calculated from the vector of the variable parameters $\underline{\theta}$, the measurement matrix $\underline{B}$ and the contraction velocity vector $\underline{v}$, deducting the damping part.

$$\underline{F}_M = \underline{B} \cdot \underline{\theta} - D \cdot \underline{v} \ . \tag{19}$$

Defining the model error as the difference between the measured force values $\underline{F}_m$ and the model force values $\underline{F}_M$

$$\underline{e}_M = \underline{F}_m - \underline{F}_M = \underline{F}_m - [\underline{B} \cdot \underline{\theta} - D \cdot \underline{v}] \ , \tag{20}$$

a quadratic performance index can be defined as

$$J(\underline{\theta}) = \underline{e}_M^T \cdot \underline{e}_M \ . \tag{21}$$

The necessary condition to obtain a minimum is a vanishing derivative

$$\frac{\partial J(\underline{\theta})}{\partial \underline{\theta}} \stackrel{!}{=} \underline{0} \ . \tag{22}$$

Solving (22) for $\underline{\theta}$, results in

$$\underline{\theta} = \left[\underline{B}^T \cdot \underline{B}\right]^{-1} \left[\underline{B}^T \cdot \underline{F}_m + D \cdot \underline{B}^T \cdot \underline{v}\right] \ , \tag{23}$$

where the product $\underline{B}^T \cdot \underline{B}$ has to be invertible.

The unknown coefficients of the volume model are determined analogously. In fig. 4 the modeled and the measured forces are compared. Fig. 5 shows a set of characteristic curves of the muscle volume including the measuring points.

3. MODELING OF THE MOTORIZED ORTHOSIS

Generally, both the patient's leg and the apparatus have to be modeled. The mechanical models of the orthosis and the patient's leg consist of four rigid bodies (fig. 6): the thigh, the knee, the shank and the foot. The thigh and the shank of the apparatus are aluminum profiles, which are assumed to be quadratic bodies, with masses $m_{th,a}$, $m_{sh,a}$ and moments of inertia $J_{th,a}$, $J_{sh,a}$. The orthosis knee joint, with the lumped mass $m_{k,a}$, connects the thigh and the shank over an arbor to which a cogwheel wound by a chain is mounted. The ends of the chain are attached to the lower ends of the pair of muscles, whereas the upper ends are fixed. At the ankle, a mechanism for stimulating the sole of the foot, which shall be referred to henceforth as the 'Stimulative Shoe', is installed. In this paper, the focus will only be put on the movement of the knee joint. The patient's foot has a mass of $m_{f,p}$ and the Stimulative Shoe has a mass of $m_{f,a}$, which can be regarded as lumped masses. While the length of each component can be varied, by adjustment, to adapt the length of each patient's leg, the hip joint is held fixed by a swivel-joint and the ankle joint is mounted on a linear bearing with low friction (fig. 6). Each leg is modeled and controlled separately. As the ankle joint is assembled on a linear bearing, the movement of the knee joint also induces a movement of the hip joint. Due to this constraint, the degrees of freedom are reduced from $f = 2$ to $f = 1$. This leads to an interdependency of the hip angle a and the knee angle q

$$a = a(q, k_1) \ . \tag{24}$$

This relation can be derived by the use of the inverse kinematics. The configuration factor k_1 takes the ambiguity of knee angles $q > 0$ into account. The thigh of the patient is modeled as a frustum ($m_{th,p}$, $J_{th,p}$), the shank as a cylinder ($m_{sh,p}$, $J_{sh,p}$). All bodies are assumed to be rigid. The equations of motion can be obtained by the use of Lagranges equations. The evaluation of

$$\frac{\partial}{\partial t}\left(\frac{\partial L}{\partial \dot{q}}\right) - \frac{\partial L}{\partial q} = Q_{nk} \ , \tag{25}$$

wherein $L = T - U$ represents the difference between the potential energy U and the kinetic energy T. The term Q_{nk} stands for the non-conservative forces. Evaluating (25) leads to the equation of motion of the form

$$m(q) \cdot \ddot{q} + k(q, \dot{q}) + G(q) = M_k - \tau \ . \tag{26}$$

In the equation of motion, $m(q)$ represents the inertial term, $k(q, \dot{q})$ contains the centrifugal and Coriolis forces, G(q) includes the gravitational terms and τ represents the disturbance torque. The masses of the patients lower limbs are computed hinging on their dependency on body weight. These bodywise-segmented inertial parameters have been estimated in [De Leva (1996)]. The required knee torque M_k is produced by a pair of DMSP-20 pneumatic muscles. With the identified force model (13), $M_k(q, \dot{q}, \ddot{q}, k_1)$ follows out of the equilibrium condition

$$M_k = \frac{d_{cw}}{2} \cdot \left(F^e(\Delta L^e, p^e) - F^f(\Delta L^f, p^f)\right) \ , \tag{27}$$

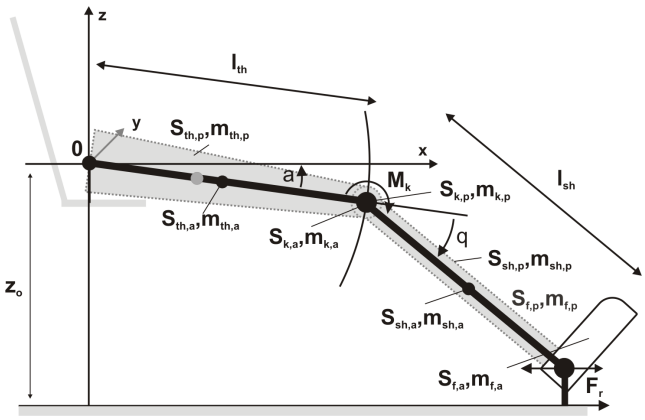

Fig. 6. Model assumptions for mechanical modeling

wherein d_{cw} stands for the cogwheel diameter, F^e_{tow} and F^f_{tow} are the force of the extensor and the flexor muscle, respectively. Since a cascaded control structure (fig. 7) is chosen, the system description for the nonlinear knee position-system can be given

$$\begin{aligned} \dot{\underline{x}}^k_{pos} &= \underline{f}(\underline{x}^k_{pos}) + \underline{C}(\underline{x}^k_{pos}) \cdot \underline{u}^k_{pos} \ , \\ \underline{x}^k_{pos} &= \begin{bmatrix} q \\ \dot{q} \end{bmatrix} \ , \ \underline{u}^k_{pos} = \begin{bmatrix} p^k_e \\ p^k_f \end{bmatrix} \ . \end{aligned} \tag{28}$$

The muscle pressure dynamics for the decoupled backstepping pressure control (fig. 7) is given in (6).

4. NONLINEAR OBSERVER

Since the velocity $\dot{q}$ of the knee angle cannot be measured, a nonlinear observer is utilized to expedite the same. Furthermore, the paralepsis of the inherent weight of the muscles and sensors, in addition to the imprecise estimation of the patients masses and model assumptions, lead to ample disturbances. Hence, the disturbance torque τ is estimated by a disturbance observer. The states

$$\underline{x}_B = [q \quad \dot{q} \quad \tau]^T \ , \tag{29}$$

shall be observed. The knee angle q can be measured and is a further input parameter into the observer

$$\underline{y}^k_{pos} = q \ . \tag{30}$$

The observer system is given by

$$\begin{aligned} \dot{\hat{\underline{x}}} &= \underline{f}(\hat{\underline{x}}, \underline{u}^k_{pos}) + \underline{h}(\hat{\underline{x}}, \underline{u}^k_{pos}) \cdot (\underline{y}^k_{pos} - \hat{\underline{y}}) \ , \\ \hat{\underline{y}} &= \underline{c}(\hat{\underline{x}}) \ , \end{aligned} \tag{31}$$

wherein $\underline{h}(\hat{\underline{x}}, \underline{u}^k_{pos})$ represents a column vector depending on the observed states $\hat{\underline{x}}$ and the control variables $\underline{u}^k_{pos}$. With the estimation error $\tilde{\underline{x}} = \underline{x}_B - \hat{\underline{x}}$ and the first-order Taylor series approximation of $\dot{\underline{x}}_B = \underline{f}(\underline{x}_B, \underline{u}^k_{pos})$, the error system is given by

$$\dot{\tilde{\underline{x}}} = \left[\frac{\partial \underline{f}}{\partial \underline{x}}(\hat{\underline{x}}, \underline{u}^k_{pos}) - \underline{h} \cdot \frac{\partial \underline{c}}{\partial \underline{x}}(\hat{\underline{x}}) \right] \cdot \tilde{\underline{x}} =: \tilde{\underline{A}} \cdot \tilde{\underline{x}} \quad . \tag{32}$$

The components of the vector $\underline{h}(\hat{\underline{x}}, \underline{u}^k_{pos})$ are specified by pole placement [Foellinger (1993)] for the system matrix $\tilde{\underline{A}}$ of the estimation error system (32). The validation of the velocity and disturbance estimation is realized in simulation. Fig. 8 shows the angle, velocity and disturbance tracking for a sinusoidal disturbance.

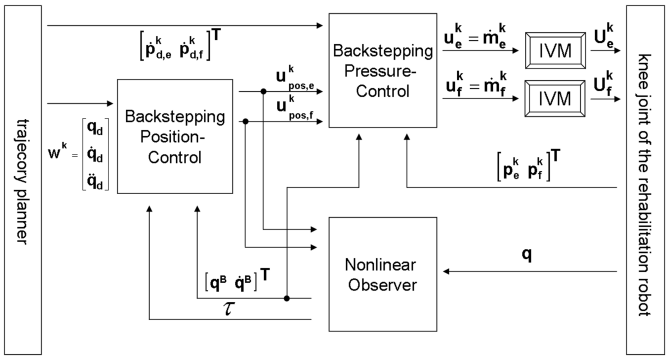

Fig. 7. Block diagram of the nonlinear observer-based control of the knee joint

5. NONLINEAR BACKSTEPPING CONTROL

The control unit design by backstepping [Knestel (2006), Aschemann et al. (to appear)] is based on the asymptotic stability theorem of Lyapunov, whereby, the complete system of order n is separated into n partial systems. Each partial system is then stabilized separately by a Control-Lyapunov-Function (CLF) $V(\underline{x}^k_{pos})$ over a new virtual input parameter, whereas the CLF has to be positive definite and its time derivative has to be negative definite. The position controller and the muscle pressure controller are implemented as a cascaded structure (fig. 7). The inner pressure of each muscle and the angle at each joint are recorded by sensors. The mass flow of air into the muscles is regulated by proportional valves. The conversion of the mass flow into the valve voltage is realized by means of an inverse valve model (IVM). As a trajectory control is desired, the rest position is the tracking error $\underline{e} = 0$. The backstepping design is exemplarily demonstrated for the position control of the knee joint. The position system description is given in (28). The error system of the first partial system is determined as follows

$$\begin{aligned} e_1 &= q_d - q \ , \\ \dot{e}_1 &= \dot{q}_d - \alpha \ , \end{aligned} \tag{33}$$

wherein α represents the new virtual input parameter. A reasonable CLF that satisfies all constraints is

$$V_1 = \frac{1}{2} \cdot e_1^2 \ . \tag{34}$$

The time derivative is dependent on the new input parameter α, by which the $\dot{V}_1 < 0$ for asymptotic stability can be enforced

$$\dot{V}_1 = e_1 \cdot \dot{e}_1 = e_1 \cdot (\underbrace{\dot{q}_d - \alpha}_{\stackrel{!}{=} -c_1 \cdot e_1}) \ . \tag{35}$$

The second partial system contains the velocity error, where the new input parameter α is the reference

$$e_2 = \alpha - \dot{q} = \underbrace{\dot{q}_d - \dot{q}}_{\dot{e}_1} + c_1 \cdot e_1 \ . \tag{36}$$

The second partial system is stabilized by a further positive definite and quadratic CLF. By fulfilling the following condition

$$\begin{aligned} \dot{V}_2 &= -c_1 \cdot e_1^2 \\ &\quad + e_2 \cdot \underbrace{(e_1 + \ddot{q}_d - \ddot{q}(\underline{u}^k_{pos}) + c_1 \cdot (e_2 - c_1 \cdot e_1))}_{\stackrel{!}{=} -c_2 \cdot e_2} \ , \end{aligned} \tag{37}$$

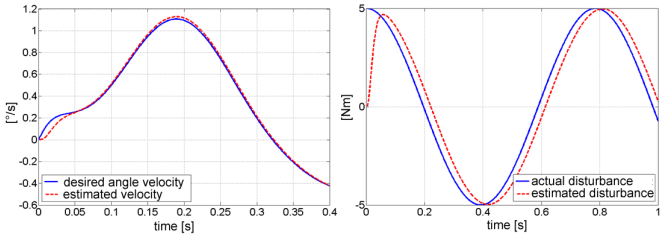

Fig. 8. Tracking performance of the nonlinear observer

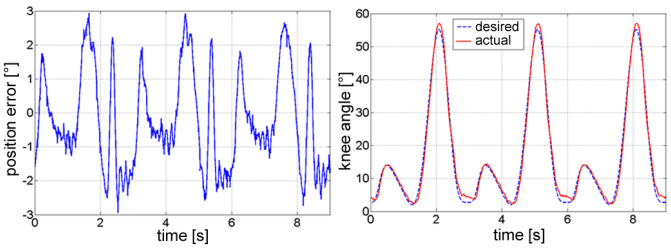

Fig. 9. Position error and tracking performance of the nonlinear backstepping controller

the control variables $u^k_{1,pos} = p^k_e$ and $u^k_{2,pos} = p^k_f$ are obtained. To achieve antagonistic muscle movement and to enable independent computation of each actuating variable, the intermediate pressure $p^k_{im} = \frac{1}{2} \cdot (p^k_e + p^k_f)$ of each pair of muscles is introduced.

6. RESULTS

The force model of the muscle, which is dependent on the inner pressure and the muscle length, is compared with the measured force in fig. 4 for varying contractions. Maximum force errors up to approximately 30 N dip below the measurement accuracy of the load cell and occur after changes in direction. The nonlinear observer exhibits an accurate estimation of the velocity and the disturbance investigated in simulation (fig. 8). After a short settling time, the velocity is estimated accurately. The disturbance prediction exhibits a small angular phase shift of approximately 25 milliseconds, which is dependent on the chosen dynamical setting. The tracking performance of the nonlinear backstepping position control is experimentally investigated for the prototype of the rehabilitation robot (fig. 1) built at the Institute of Measurement, Control, and Microtechnology of the University of Ulm. For the measurement, the apparatus has been operated without a test person. Maximum tracking errors of approximately 3 degrees are found to occur during maximum acceleration and deceleration, particularly during the swing phase (fig. 9). The steady-state error at the beginning of the step is less than 1 degree. The desired trajectory of the knee angle is obtained by fitting it to the mean knee angle trajectory of ten healthy persons. This data has been provided by the Orthopedic University Hospital II of Heidelberg.

7. CONCLUSION

In this paper, the volume and force modeling of pneumatic artificial muscles of the type DMSP-10 and DMSP-20 is presented. The model description is derived by use of polynomial approaches, whose coefficients are dynamically identified in a test rig depicted in fig. 2. The investigated muscle is held on constant pressure, while a forceful positioning muscle varies its contraction and the applied force to induce the movement is measured. In order to demonstrate the applicability of the pneumatic artificial muscle, a nonlinear observer based backstepping controller is derived. For this, the mechanical model of the partial system of the knee joint is deduced. The observer compensates disturbances caused by friction, model uncertainties or unpredictable patient movements with an acceptable angular phase shift that bears a dependency on stipulated error dynamics. Due to its stability-oriented design, the controller demonstrates high robustness at adequate accuracy. The inevitable high complexity of model based control is justified by the many advantages of the use of muscles in this application, e.g. simple safety concept owing to their elasticity and relocatability when depressurized, soft and tractable control, low weight, high dynamics and low price.

REFERENCES

H. Aschemann and E. P. Hofer. Flatness-based trajectory control of a pneumatically driven carriage with model uncertainties. In *Proceedings of NOLCOS, Stuttgart, Germany*, 2004.

H. Aschemann, M. Knestel, and E.P. Hofer. Nonlinear control strategies for a parallel robot driven by pneumatic muscle actuators. In *Proceedings of the 14th Workshop on Dynamics & Control, Moskow, Russia*, to appear.

G. Colombo, M. Wirz, and V. Dietz. Driven gait orthosis for improvement of locomotor training in paraplegic patients. *Spinal Cord*, 39:252–255, 2001.

P. De Leva. Adjustments to zatsiorsky-seluyanovs segment parameters. *Journal of Biomechanics*, 29:1223–1230, 1996.

V. Dietz, G. Colombo, L. Jensen, and L. Baumgartner. Locomotor capacity of spinal cord in paraplegic patients. *Ann Neurol*, 37:574–82, 1995.

V. Dietz, R. Mueller, and G. Colombo. Locomotor activity in spinal man: significance of afferent input from joint and load receptors. *Brain*, 125:2626–34, 2002.

O. Foellinger. *Nichtlineare Regelungen II.* R. Oldenburg Verlag Mnchen, 1993.

K. Gordon, G. Sawicki, and D. Ferris. Mechanical performance of artificial pneumatic muscles to power an ankle foot-orthosis. *Journal of Biomechanics*, 39:1832–1841, 2006.

H. Herr and R. Kornbluh. New horizons for orthotic and prosthetic technology: artificial muscle for ambulation. *Proceedings of SPIEs Smart Structures and Materials 2004*, Vol. 5385 (2004):1–9, 2004.

S. Hesse, C. Bertelt, and M.T. et al.: Jahnke. Treadmill training with partial body weight support compared with physiotherapy in nonambulatory hemiparetic patients. *Stroke*, 26:976–981, 1995.

S. Klee Barillas. *Identifikation, Modellbildung und nichtlineare Regelung des Kniegelenks eines durch pneumatische Muskeln angetriebenen Beintrainers.* Diploma thesis, University of Ulm, 2007.

M. Knestel. *Modellgestuetzter nichtlineaer Regelungs- und Beobachterentwurf fuer einen hochdynamischen Parallelroboter.* Diploma thesis, University of Ulm, 2006.